Received 22 October 2023; revised 18 January 2024; accepted 23 February 2024.
Date of publication 20 March 2024; date of current version 2 April 2024.

Digital Object Identifier 10.1109/OAJPE.2024.3379485

Decentralized Reactive Power Control in Distribution Grids With Unknown Reactance Matrix

LINTAO YE[1] (Member, IEEE), KRISHNA CHAITANYA KOSARAJU[2] (Member, IEEE), VIJAY GUPTA[3] (Fellow, IEEE), RODRIGO D. TREVIZAN[4] (Member, IEEE), RAYMOND H. BYRNE[4] (Fellow, IEEE), AND BABU R. CHALAMALA[5] (Fellow, IEEE)

[1]School of Artificial Intelligence and Automation, Huazhong University of Science and Technology, Wuhan 430074, China
[2]Department of Electrical Engineering, University of Notre Dame, Notre Dame, IN 46556 USA
[3]Elmore Family School of Electrical and Computer Engineering, Purdue University, West Lafayette, IN 47907 USA
[4]Energy Storage Technology and Systems Department, Sandia National Laboratories, Albuquerque, NM 32611 USA
[5]Nuclear Fuel Cycle and Grid Modernization Center, Sandia National Laboratories, Albuquerque, NM 32611 USA

CORRESPONDING AUTHOR: V. GUPTA (gupta869@purdue.edu)

This work was supported in part by U.S. Department of Energy, Office Electricity, Energy Storage Program; and in part by the National Technology & Engineering Solutions of Sandia LLC with U.S. Department of Energy (DOE) under Contract DE-NA0003525. The work of Lintao Ye was supported in part by the NSFC under Grant 62203179.

ABSTRACT We consider the problem of decentralized control of reactive power provided by distributed energy resources for voltage support in the distribution grid. We assume that the reactance matrix of the grid is unknown and potentially time-varying. We present a decentralized adaptive controller in which the reactive power at each inverter is set using a potentially heterogeneous droop curve and analyze the stability and the steady-state error of the resulting system. The effectiveness of the controller is validated in simulations using a modified version of the IEEE 13-bus and a 8500-node test system.

INDEX TERMS Decentralized control, energy storage, power distribution systems, volt/VAr control.

I. INTRODUCTION

DISTRIBUTED Energy Resources (DERs), including both renewable energy resources and energy storage devices, are changing the paradigm of power generation, transmission and distribution. In traditional distribution networks (DNs), load variations over time cause fluctuations in voltage due to a mismatch between reactive power supplied and consumed. Such voltage fluctuations are typically mitigated through the use of switched capacitor banks and step voltage regulators. As the adoption of DERs increases, and as consumers both produce and consume energy, often referred to as prosumers, the time-varying, intermittent, and unpredictable changes in load and generation will lead to even larger voltage fluctuations. Consequently, traditional voltage regulation devices must operate more frequently, which may reduce operational life of those devices and increase maintenance costs [1], [2].

However, the inverters that connect these DERs to the distribution network are flexible power electronic converters that are capable of controlling the reactive power they inject into the DN independently of the real power injection, potentially allowing for mitigation of voltage deviations through reactive power compensation. Several algorithms, both centralized and local, have been proposed to identify control strategies for such inverters [3], [4], [5], [6], [7], [8]. Within the class of local controllers, we can distinguish between distributed controllers [9], [10], [11], [12], [13], which require neighboring inverters to communicate with each other, and decentralized controllers [14], [15], [16] that do not require any information exchange. In this paper, we focus on the latter.

For decentralized control, a common practice (e.g., used in IEEE 1547 standard) is to use volt/VAR droop curves to determine the reactive power injected (or absorbed) by the inverters into the power grid [17], [18], [19], [20], [21], [22], [23], [24]. These local droop controllers do not require communication among themselves to operate effectively, can operate in parallel, and can operate within the hierarchical voltage control scheme of distribution networks. However, a known disadvantage of such droop controllers is that they naively do not consider the effect of the droop controllers present at other nodes. Since the entire distribution network is dynamically coupled, droop controllers at various nodes can interact among themselves in a way that can lead to them failing to deliver the required power quality and even resulting in stability loss for the entire network that manifests itself as steady-state oscillations in the voltage [17], [25]. If the droop gain is lowered, the effects of interactions are mitigated, but larger steady state voltage error will result.

To overcome this issue, several techniques have been proposed. Early contributions provided a rigorous stability analysis by modelling the distribution system in continuous time [26]. Because of the fast action response of the inverter based DERs, [27] argues that a discrete time formulation is more appropriate to model the problem and supplements the droop curve with a first-order filter. A popular line of work [17], [24], [28] is to develop a small-signal based stability analysis by assuming that the system operates in the linear region of the droop curves. In [29], the authors identify the stability conditions by assuming that the same controller is being utilized at all nodes.

Since the distribution network is dynamically coupled, it is not surprising that all the above proposed techniques require the knowledge of the reactance matrix of the distribution network for analysis and controller design (with sufficient analysis conditions possible through a metric such as the norm or the spectral radius of the matrix). This matrix is used as part of an affine or linearized model that maps the changes in the node power injections to the nodal voltage deviations. The nodal reactance depends on factors such as the power injected through the DERs, the power consumed by the loads at each node, and the topology of the distributions system. Distribution networks are typically insufficiently monitored and model and parameter errors are very common [30]. Thus, accurate knowledge of the reactance matrix is usually an onerous assumption. Metrics such as spectral radius can be very sensitive to precise values of the parameters or the model. Further, most of these works assume that the reactance matrix is time-invariant, which implies that the factors listed above (such as the power injected through the DERs or consumed at the loads) are time-invariant. This can limit the applicability of the analysis or at least make it conservative as the number of prosumers increases and changes in the distribution network become more frequent.

We take a step towards a decentralized controller design to guarantee voltage stability of a distribution network with multiple inverters when the reactance matrix may be unknown and time-varying. We consider a discrete-time formulation and allow for heterogeneous droop curves at the inverters. We begin by presenting a decentralized controller to control the reactive power injection (or absorption) at each node as a function of the local voltage. As in the case of most existing techniques, ensuring stability with such a controller requires the knowledge of the reactance matrix to design the droop curves. Our main result is to utilize the structure of this controller to design an adaptive controller that does not require this knowledge for the case when the reactance matrix is unknown and possibly time-varying. The adaptive controller requires a small dither signal to probe the network in order to ensure that the controller converges to a neighborhood of the desired value, thus resulting in a small steady-state error. We provide tuning rules to decrease the steady-state error while maintaining stability of the overall network. Some of the results in this paper were presented in an initial form in [31]. As compared to that paper, we present a proof of the convergence of the proposed adaptive controller, analyze the steady-state error introduced by the controller, and present more detailed simulation studies including on an 8500-node system.

We begin by presenting the system model in Section II. We first present an initial dissipativity-based design of the controller. For the case when the reactance matrix is unknown and time-varying, we then present an adaptive extremum-seeking approach to converge to the correct controller. Some numerical case studies are presented in Section IV.

II. SYSTEM MODEL

Consider a radial distribution network with $n+1$ buses numbered as $0, 1, \cdots, n$. Without loss of generality, bus 0 is the substation bus assumed to be at a fixed voltage. Define the set of buses by $\mathcal{N} \triangleq \{0, 1, \ldots, n\}$. Denote the set of lines connecting the buses by $\mathcal{L}$ with the line $(i, j) \in \mathcal{L}$ connecting buses i and j. For each bus $i \in \mathcal{N}$, denote the magnitude of the voltage at this bus by v_i, the real power injection by p_i and the reactive power injection by q_i (with injection denoted by a positive value and absorption by a negative sign). Denote the stacked vectors of these quantities at all the buses by v for the voltage magnitudes, p for the real power injections, and q for the reactive power injections.

In a distribution grid, the voltage magnitude v can be observed and the reactive power injections q can be controlled. We are interested in decentralized control, so that the reactive power injections at each node must be controlled locally. We follow the development of [27] to describe the dynamics of the system. For simplicity, we consider a single-phase grid although the basic idea presented here can be extended to three-phase systems. We assume that the dynamics of the grid are considered in a discrete-time fashion with the discretization time T_s that is sufficiently large so that the power system dynamics (grid, load, and inverter dynamics) reach a steady state between the discrete-time steps. Thus, if the reactive power injections $q(k)$ are specified at time step k, then the actual injections will reach these values at time step $k+1$. Further, the corresponding voltages (given by the power flow equations) will also reach a steady state at time step $k+1$. We assume that the voltages are obtained through a linearization of the nonlinear power flow equations at 1 pu.

If we denote the *prescribed values* of the reactive power injections at iteration k by the control input $u(k)$, and assume that the voltages $v(k)$ can be observed, then the above discussion can be summarized in a system model of the form

$$\Sigma_l: \quad \begin{aligned} q(k+1) &= u(k) \\ y(k) &= v(k), \end{aligned} \tag{1}$$

with the voltage $v(k)$ and reactive power $q(k)$ satisfying $v(k) = Xq(k) + \tilde{v}$, where X is a positive definite matrix that characterizes the reactance of the network and $\tilde{v}$ is a vector that depends on the real power injections and the resistances in the network and is not controllable. This linearized model is widely accepted, see, e.g., [27], [29], [32], [33], and [34]. While it is usually assumed for convenience that X is a constant matrix, its value depends on factors such as the power injected through the DERs, the power consumed by the loads at each node, and the topology of the distributions system. Especially as DER penetration increases, the validity of this assumption quickly degrades. In this paper, we seek to relax this assumption, so that we denote the value of the matrix at time k by $X(k)$. We assume that $X(k)$ is chosen from a set $\mathcal{X}$. Further, the precise value of $X(k)$ is often unknown since distributions networks are usually under-monitored.

We aim to design the control input $u(k)$ as a causal function of the output $y(0), \cdots, y(k)$, so that the voltage $v(k)$ locally asymptotically stabilizes to a desired setpoint $v^\star$. Further, it should be a local controller in the sense that each input $u_i(k)$ depends only on the local outputs (or voltages) at bus i. Finally, the control input $u(k)$ must satisfy the physical limits of the reactive power that can be supplied or absorbed by the inverter, so that $u(k) \in [q_{\min}, q_{\max}]$. For ease of notation, we assume that the saturation limits $q_{\min}$ and $q_{\max}$ are fixed and constant for every inverter, although our arguments below can be generalized.

Let the voltage setpoint of the system Σ_l be denoted as $v^\star$. For a given matrix X, the corresponding reactive power setpoint is given by $v^\star = Xq^\star + \tilde{v}$, with $q^\star \in [q_{\min}, q_{\max}]$. Denote the set of all feasible operating points by

$$\mathcal{C} = \left\{(q, v) \in \mathbb{R}^n \times \mathbb{R}^n | v = Xq + \tilde{v}\right\}. \quad (2)$$

Finally, denote the incremental quantities $\Delta q(k) = q(k) - q^\star$, $\Delta u(k) = u(k) - u^\star$, and $\Delta v(k) = v(k) - v^\star$.

III. PROPOSED CONTROLLER DESIGN

Our controller builds on two basic ideas. In Section III-A, we begin by designing a controller that ensures convergence to the correct setpoint if the reactance matrix were perfectly known. We achieve this through the notion of dissipativity. Then, in Section III-B, we extend this design to present an adaptive controller that achieves convergence to the setpoint even when the reactance matrix is not known. We achieve this through an extremum-seeking controller.

We begin with the first part now. As mentioned above, our controller design is based on the system-theoretic notion of dissipativity. For a detailed treatment of dissipativity, we refer the reader to books such as [35]; a brief overview is provided in Appendix A. Beginning from energy dissipation through resistors in electrical circuits, the notion of dissipativity formalizes the notion of energy being dissipated in a system that is being supplied energy from external inputs. A dissipativity-ensuring controller ensures that the closed-loop system dissipates energy by imposing that the energy supplied externally (measured using a supply rate) is more than the energy stored by the system (measured using a storage function). Such a property naturally ensures that the system is stable. By considering the error system with respect to a setpoint, we can easily translate such stability to convergence to a desired setpoint. Dissipativity-based control has been extensively used, including in power grids.

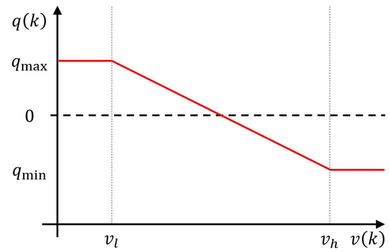

FIGURE 1. Sample volt/VAr droop control characteristic.

We begin by presenting a dissipativity property for the linearized system Σ_l. Using that, we design a new dissipativity-based controller to ensure that the voltage set point is asymptotically stable. The dissipativity analysis of the system Σ_l is slightly complicated by the fact that the input $u(k)$ is related to $q(k+1)$ and hence the output $y(k+1)$ at time $k+1$. We use the well-known tool of scattering transformations used in the theory of dissipativity of time-delay systems [36]. Specifically, we use the scattering transform defined by

$$\nu(k) = \Delta v(k) + X(k+1)\Delta u(k), \quad (3a)$$

$$\omega(k) = -\Delta v(k) + X(k+1)\Delta u(k). \quad (3b)$$

We can then prove the following result.

Lemma 1: The system Σ_l is dissipative with respect to the input $\nu(k)$ and output $\omega(k)$ irrespective of how $u(k)$ is designed.

Proof: Consider the storage function $S(k) = \|X(k)\Delta q(k)\|_2^2$. Then, we can write

$$\begin{aligned}
&S(k+1) - S(k) \\
&= \|X(k+1)\Delta q(k+1)\|_2^2 - \|X(k)\Delta q(k)\|_2^2 \\
&= \|X(k+1)\Delta u(k)\|_2^2 - \|\Delta v(k)\|_2^2 \\
&= (\Delta v(k) + X(k+1)\Delta u(k))^\top (-\Delta v(k) + X(k+1)\Delta u(k)) \\
&= \nu(k)^\top \omega(k),
\end{aligned}$$

which concludes the proof. ■

We emphasize that the dissipativity above has been proven with respect to a 'dummy' input $\nu(k)$ and output $\omega(k)$ and holds irrespective of the controller used to design $u(k)$.

A. CONTROL Design

We now show that the dissipativity property proved above can be utilized to design a controller that stabilizes the system around the desired setpoint. Specifically, consider the following controller inspired by the popular droop controllers and shown in Fig. 1:

$$u(k) = \begin{cases} q_{\max} & v(k) < v_l \\ u^\star - \overline{K}\left(v(k) - v^\star\right) & v_l \leq v(k) \leq v_h \\ q_{\min} & v(k) > v_h, \end{cases} \tag{4}$$

where q_{max} and q_{min} denote the maximum and the minimum allowed reactive power injections and $\overline{K} \in \mathbb{R}^{n\times n}$ is a diagonal matrix representing the slope of the droop curve. Further, for the system not to have a trivial equilibrium in the saturated regime, we assume that the parameters $v_l \in \mathbb{R}^n$ and $v_h \in \mathbb{R}^n$ are chosen to satisfy

$$v_h \geq X(k)q_{\max} + \tilde{v} \geq v_l \tag{5}$$
$$v_l \leq X(k)q_{\min} + \tilde{v} \leq v_h, \tag{6}$$

for all allowed matrix values $X(k) \in \mathcal{X}$. These relations can be interpreted as imposing constraints on the allowed voltage range as a function of the reactive power capacity of the DERs so that stability can still be guaranteed.

The following result is proven in Appendix B.

Theorem 1: Consider the system Σ_l with the controller (4). Let $\overline{K}$ be a diagonal matrix that satisfies the condition

$$K(k) := (I + X(k)\overline{K})^{-1}\left(X(k)\overline{K} - I\right) < 0 \tag{7}$$

such that $K(k) + K^T(k)$ is negative-definite for all $X(k) \in \mathcal{X}$. Then:

(i) The closed loop system is dissipative with respect to the supply-rate $w(\omega) := \omega^\top(k)K(k)\omega(k)$.

(ii) Assume further that $X(k)$ asymptotically converges to a value $\overline{X}$. Then the closed loop system is asymptotically stabilized to the desired operating point $(q^\star, v^\star)$ corresponding to the voltage set point $v^\star$ and the corresponding reactive power given by $v^\star = \overline{X}q^\star + \tilde{v}$, with $q^\star \in [q_{\min}, q_{\max}]$.

Theorem 1 proves the stability of a controller inspired by the droop controller, under some conditions on the range of the linear portion of the controller (given by (5) and (6)) and restrictions on the slope of the linear portion of the controller with respect to the matrix X of the distribution grid. Note that the dissipativity result (part (i)) holds even if the matrix X is time varying. For asymptotic stability to hold in part (ii), we naturally require the dynamic system to become time invariant and thus the reactance matrix has to eventually converge.

B. ADAPTIVE CONTROLLER

Although the controller (4) is sufficient to stabilize the system Σ_l, it requires the knowledge of the desired setpoint $u^\star$, which, in turn, requires the value of the matrix $\overline{X}$. Obtaining the values of this matrix accurately in a distribution grid is often not possible in practice. To overcome this limitation, we now propose an adaptive controller that does not require any knowledge of $u^\star$. We continue to assume that the condition $\lim_{k\to\infty} X(k) = \overline{X}$ holds.

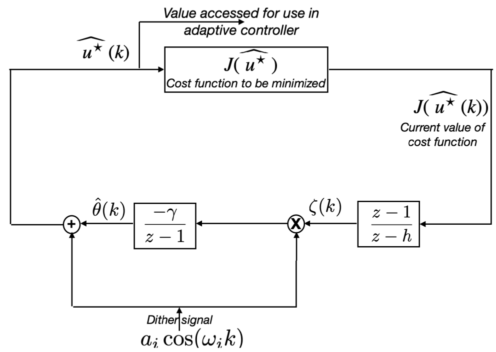

FIGURE 2. Proposed algorithm for identifying $\widehat{u^\star}(k)$.

Following the theory of extremum-seeking controllers (ESCs) [37] the controller at time k is of the form:

$$u(k) = \widehat{u^\star}(k) - \overline{K}\left(v(k) - v^\star\right), \tag{8}$$

where $\widehat{u^\star}(k) \in \mathbb{R}^n$ denotes the current estimate of the unknown desired reactive power $u^\star$. Note that this controller is of the same form as the proposed controller in (4) with the (unknown) term $u^\star$ replaced by its current estimate $\widehat{u^\star}(k)$. To update $\widehat{u^\star}(k)$, we follow the design in Fig. 2. Since $u^\star$ corresponds to the desired setpoint $q^\star$ of the reactive power, we define a cost function $J(\widehat{u^\star}(k))$ associated with any choice of $\widehat{u^\star}(k)$ as

$$J(\widehat{u^\star}(k)) = \|\overline{X}u(k) + \tilde{v} - v^\star\|_2^2. \tag{9}$$

This cost function is zero precisely when $\widehat{u^\star}(k)$ equals $u^\star$. The ESC theory updates the term $\widehat{u^\star}(k)$ in a manner such that asymptotically, the cost function is driven to zero. More specifically, as proposed in [37], we update the estimate as

$$\widehat{u_i^\star}(k+1) = \widehat{\theta}_i(k+1) + a_i\cos(2\pi\alpha_i(k+1)) \tag{10}$$
$$\widehat{\theta}_i(k+1) = \widehat{\theta}_i(k) - \gamma_i a_i\cos(2\pi\alpha_i k)\left(J(\widehat{u^\star}(k)) - (1+h)\zeta(k)\right) \tag{11}$$
$$\zeta(k) = -h\zeta(k-1) + J(\widehat{u^\star}(k-1)), \tag{12}$$

where $\zeta(k)$ is a scalar and the subscript i indicates the i-th vector entry. The signal $a_i\cos(\omega_i k)$ is a dither signal with a small amplitude a_i and frequency $\alpha_i = \frac{\omega_i}{2\pi}$, with $0 < \alpha_i < 1$. γ_i is the adaptation gain chosen such that $\frac{\gamma_i a_i^2}{2} < 1$. The high-pass filter $\frac{z-1}{z+h}$ is designed with $0 < h < 1$ and a cutoff frequency well below $2\pi\alpha_i$. The ESC is a gradient-based controller and thus any convergence result is necessarily local. Thus, we assume that the the system Σ_l remains in the linear range of the controller (4). We can then show the following result proven in Appendix C.

Theorem 2: Consider the system Σ_l in closed loop with the controller of the form (8) such that $v_l \leq v(k) \leq v_h$ at every step. Let the parameter $\widehat{u^\star}(k)$ in the controller be chosen according to the equations (10)-(12). Then, it holds that the parameter $\widehat{u^\star}(k)$ locally exponentially converges to an $O(a_i)$ neighborhood of the correct value $u^\star$.

The above result proves exponential convergence of the parameter $\widehat{u^\star}(k)$ to a value $\overline{u}$ that is in a neighborhood of $u^\star$. Thus, for the case of a time-varying matrix X that may change suddenly and potentially large amounts; however remains constant for sufficiently long intervals to allow the adaptive controller to converge, the extremum-seeking controller can be utilized to ensure that the system remains in a small neighborhood of the desired set point.

C. STEADY-STATE ERROR

The choice of the parameter $\overline{K}$ has not yet been fixed beyond the condition imposed in (7). Theorem 2 indicates that the parameter $\widehat{u^\star}(k)$ used in the proposed controller (4) converges to a value $\overline{u}$ which is in a neighborhood of $u^\star$. Thus, while the controller may be stabilizing (following Theorem 1), there may be a steady-state error in the values of the voltages being tracked. The choice of $\overline{K}$ can be utilized to minimize this steady-state error as discussed below.

The reason for this steady-state error can be understood by utilizing the controller (4) with the parameter $\overline{u}$ from the ESC in the system Σ_l. The closed-loop system is written as

$$\begin{aligned} q(k+1) &= \overline{u} - \overline{K}\left(v(k) - v^\star\right) \\ v(k+1) &= \bar{X}q(k+1) + \tilde{v} \\ &= \overline{X}u^\star + \tilde{v} - \overline{XK}\left(v(k) - v^\star\right) + \overline{X}(\overline{u} - u^\star). \end{aligned}$$

At steady state, we have that $v(k+1) = v(k) = \overline{v}$ that may not necessarily be the desired setpoint $v^\star$. In fact, the steady-state error is given by

$$v_{ess} = \|v^\star - \overline{v}\|_2 = \|(I + \overline{XK})^{-1}X(u^\star - \overline{u})\|_2, \tag{13}$$

where $\|\cdot\|_2$ denotes the 2-norm of a vector. To mitigate this error, we can utilize the parameter $\overline{K}$. From (13), the reason for the steady-state error is that there is a mismatch between the terms $\overline{u}$ and $u^\star$. Thus, we define the *sensitivity* $\mathcal{S}$ of the system Σ_l with respect to the controller gain $\overline{K}$, when the controller (4) with the ESC described above is used as

$$\mathcal{S} = \max_{\overline{K}, \|\overline{X}(u^\star - \overline{u})\|_2 = 1} \frac{v_{ess}}{\|\overline{X}(u^\star - \overline{u})\|_2}. \tag{14}$$

If a is the smallest singular value of $I + \overline{XK}$, then $a > 0$ and $\frac{1}{a}$ is the largest singular value of $(I + \overline{XK})^{-1}$. Thus, by definition, the sensitivity $\mathcal{S}$ is given by

$$\mathcal{S} = \max_{\overline{K}, \|\overline{X}(u^\star - \overline{u})\|_2 = 1} \|(I + \overline{XK})^{-1}\overline{X}(u^\star - \overline{u})\|_2 = \frac{1}{a}.$$

Thus, for small steady-state error, we should choose $\overline{K}$ such that the smallest singular value of $\overline{XK}$ is as large as possible (while ensuring stability with (7)). If the matrix K is symmetric, we can also see that from Theorem 1, every eigenvalue λ of K is negative. Further, if $\overline{XK}$ is symmetric, its singluar values are the same as its eigenvalues. Thus, every eigenvalue $\frac{1+\lambda}{1-\lambda}$ of $\overline{XK}$ is in the interval $(-1,\ 1)$. Therefore, in this case, for a small steady-state error we should choose the matrix $\overline{K}$ such that the smallest eigenvalue of $\overline{XK}$ approaches 1. A numerical illustration is provided for the IEEE 13-bus test feeder example discussed further in Section IV in Figure 3, where the sensitivity of the system is plotted as a function of the smallest eigenvalue of the matrix $\overline{XK}$ for different choices of $\overline{K}$. The figure confirms that the sensitivity is the lowest when the smallest eigenvalue of $\overline{XK}$ approaches unity.

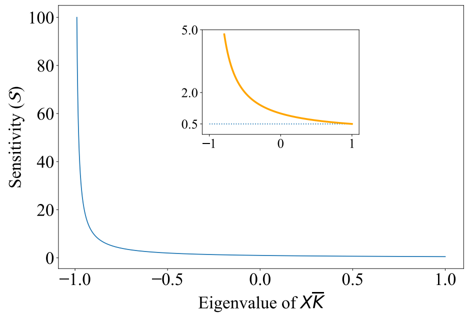

FIGURE 3. Numerical illustration of sensitivity of the IEEE 13-bus test feeder example with ESS at Buses 680 and 675 as a function of the smallest eigenvalue of the matrix $\overline{XK}$ for different choices of $\overline{K}$.

TABLE 1. Summary of test systems used in case studies.

Case	ESS Buses	ESS Power	Solar PV
13-Bus	680, 675	600 kVA	3 MW (bus 671)
8500-Node	A-G (7)	300 kVA	No

IV. CASE STUDIES

This section provides case studies to demonstrate the effectiveness of the proposed method. The first case study uses a modified version of the IEEE 13-bus test feeder to compare three voltage control systems: i) traditional voltage regulation devices, i.e., capacitor banks and on-load tap changers (OLTCs), ii) droop control of ESS is added to i), and iii) the proposed controller modulates the power injection of ESS in combination with i). A second case study is implemented using the much larger IEEE 8500-Node Distribution system to demonstrate that the proposed controller is effective on a larger-scale problem. All numerical studies are simulated using OpenDSS [38]. Relevant features of the case studies are summarized in Table 1.

A. CASE: IEEE 13-BUS TEST FEEDER

The first test case considers a simulation with a time step of 1 second over 24 hours. A 3 MW three-phase solar array was added to bus 671 to represent a utility-scale solar PV array. The power injection profile was derived from the high variability solar irradiation dataset from the Alderville site [39]. Two three-phase 600 kVA ESSs were added to the unbalanced IEEE 13-bus test feeder's buses 680 and 675, as shown in Fig. 4. The inverters have a circular capability curve. At

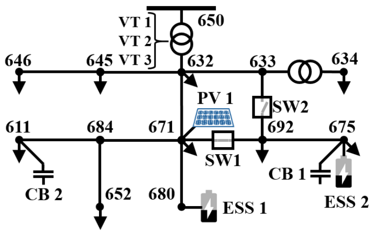

FIGURE 4. **IEEE 13-bus test feeder. Buses 680 and 675 have ESS.**

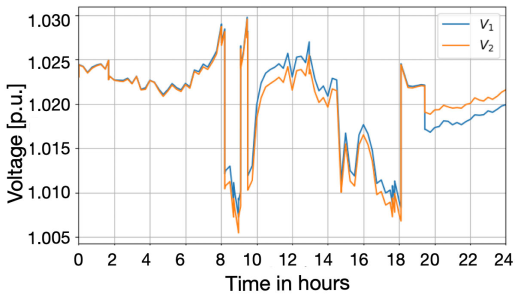

FIGURE 5. **Control system 1: Voltage profile measured by ESS 1 (V_1) and ESS 2 (V_2).**

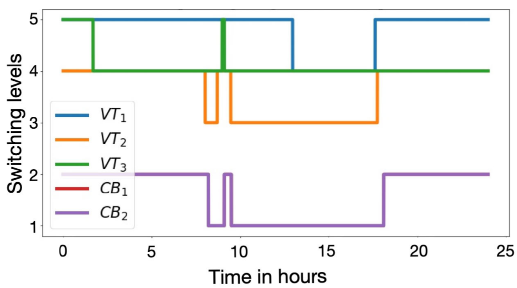

FIGURE 6. **Control system 1: Operation of capacitor banks (CB) and step-voltage regulators (VT).**

7:26 PM a system reconfiguration occurs, where SW1 opens and SW2 closes. The ESS and PV can provide volt/VAr regulation to the feeder to mitigate the voltage fluctuations caused by time-varying loads, reconfiguration of feeder, and solar generation. We consider three scenarios.

1) VOLTAGE CONTROL SYSTEM 1 (TRADITIONAL VOLTAGE REGULATORS)

This voltage control system considers that the voltage is regulated exclusively by two capacitor banks at buses 675 (CB 1, three-phase) and 611 (CB 2, single-phase), and three single-phase step-voltage regulators situated between buses 650 and 632. In this case, the ESS are inactive. Fig. 5 and Fig. 6 present the resulting voltage profiles and the switching pattern used by capacitor banks and voltage regulators. While the average voltage across the three phases is within 5% of 1 [p.u.], there are undesirable fast voltage variations and switching in capacitor banks and step-voltage regulators in the periods of fast reduction in solar generation due to clouding (between

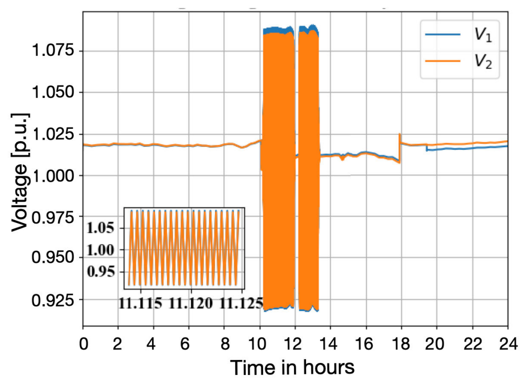

FIGURE 7. **Control system 2: Voltage oscillation introduced by the volt/VAr droop controller.**

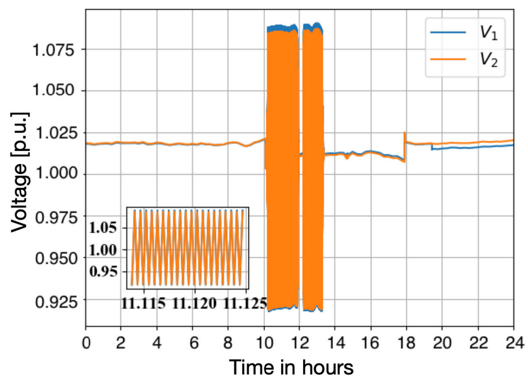

FIGURE 8. **Control system 2: Reactive power injection oscillation introduced by the volt/VAr droop controller.**

9 and 10 AM). Note that, while capacitor banks and step-voltage regulators do provide voltage control, their frequent operation is undesirable due to additional maintenance costs and decreased equipment life.

2) VOLTAGE CONTROL SYSTEM 2 (TRADITIONAL VOLTAGE REGULATORS PLUS ESS USING DROOP-BASED VOLT/VAR)

In the second voltage control system, the volt/VAR droop control capabilities of both the ESS and the PV are used. The voltage-reactive power controller settings were chosen within the range of allowable settings of standard IEEE 1547-2018 type A. Similarly to what is shown in the motivational example of [27], oscillations in the voltage and output of the volt/VAR droop controller is found when solar PV output increases, as shown in Figs. 7 and 8. The controllers saturate at every time step and introduce an oscillation in power flows and voltage of the distribution feeder. The detail plot in Fig. 8 provides a clearer idea of how those oscillations occur.

3) VOLTAGE CONTROL SYSTEM 3 (TRADITIONAL VOLTAGE REGULATORS PLUS PROPOSED ESS CONTROLLER)

In the third scenario, the proposed controller is used. The proposed controller (18) was designed using $\overline{K}$ =

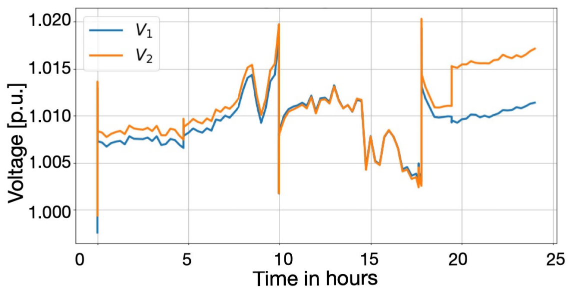

FIGURE 9. Control system 3: Voltage profile with proposed controller.

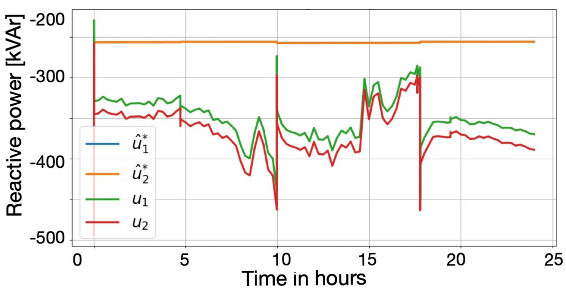

FIGURE 10. Control system 3: Power injections obtained with the proposed controller. The sharp changes at $t = 10, 17$ h correspond to the switching capacitor bank actions shown in Fig 11.

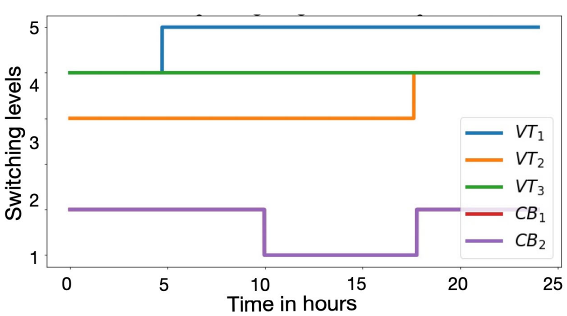

FIGURE 11. Scenario 3: Switching in Capacitor-Banks (CB) and Step-Voltage Transformers (VT) with ESC.

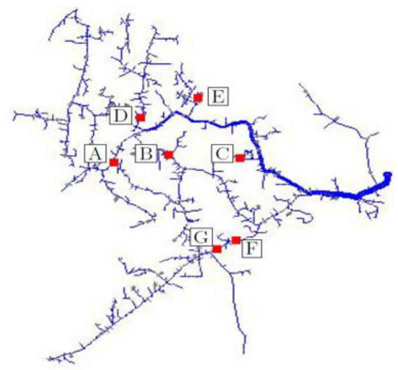

FIGURE 12. The highlighted buses of the IEEE 8500 system have ESS.

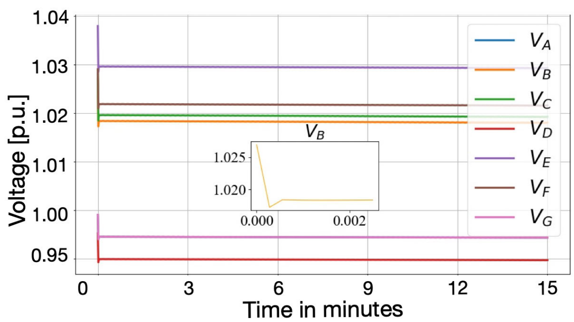

FIGURE 13. Voltage profile with proposed controller.

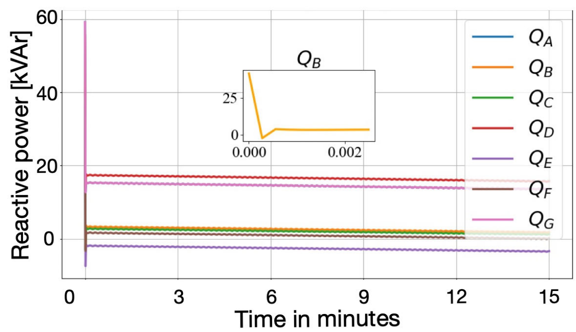

FIGURE 14. Power injections obtained with the proposed controller.

$diag\{10000, 1000\}$, which resulted in a negative definite K and which was determined through some trial and error to achieve a reasonable average voltage error. The parameters of the adaptive controller were chosen as $a_i = 0.1$, $\omega_i = \pi/2$, $\gamma_i = 0.027$, $h = 0.99$. The controller stabilizes the voltages, as shown in Fig. 9 with the power injections shown in Fig. 10.

The ESC provides the desired controller outputs, $u^\star$ shown in Fig. 10. Following a brief transient, when these controllers obtain a stable $u^\star$, which provides the first term at the right hand side of (18). When added to the second term of the same equation, we obtain the controller outputs $\widehat{u^\star}$. We notice that those act to counter the voltage fluctuations in the feeder, providing good voltage regulation by maintaining voltage very close to the target of 1 p.u. It is also important to highlight that the parameters chosen plus the actuation of the adaptive controller avoid saturation of the actuator, i.e., the reactive power absorption capability of the two ESS units. Finally, Fig. 11 depicts the behaviour of the step-voltage regulators and capacitor banks. When compared to the first scenario (Fig. 6) we see that the number of switching events is considerably reduced.

B. CASE: IEEE 8500-NODE DISTRIBUTION SYSTEM

The voltage controller was validated in a simulation with a time step of 5 seconds over 15 minutes. 6 three-phase 300 kW ESS, namely A, B, C, D, E, F, and G, were added to the IEEE 8500-node distribution system, as shown in Fig. 12. The

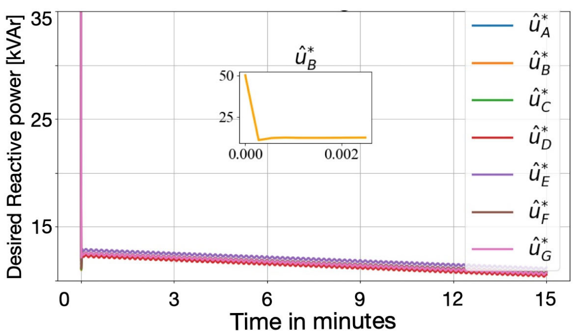

FIGURE 15. $u^\star$ estimated by the ESC for IEEE 8500 system.

volt/VAr control settings were chosen in the limits in IEEE 1547-2018 for Type A inverter. Similarly to the previous case, oscillations are detected due to the interactions of all volt/VAR controllers. implemented by ESS.

The proposed controller (18) was implemented with the proportional gain $\overline{K} = 500 \times diag\{1, 1, 1, 1, 1, 1\}$. The term $u^\star$ in (18) is estimated using the ESC (10)-(12), where the parameters of the ESC were chosen as $a_i = 0.1$, $\gamma_i = 0.1$, $h = 0.1$ and $\omega_i = \pi/5$. As shown in Figs. 13 and 14, the proposed controller is able to eliminate the oscillations of volt/VAR controllers, providing a flat voltage and reactive power profiles. Furthermore, the controller is able to maintain the voltages reasonably close to 1 p.u.

V. CONCLUSION

We provided a dissipativity-based adaptive controller for decentralized control of reactive power from DERs in the distribution grid. Importantly, we explicitly allow the reactance matrix of the grid to be unknown and even time-varying. We also provided analytical expressions to evaluate and reduce the steady-state error of voltages with the proposed controller. The controller was demonstrated through simulations in two IEEE test distribution systems modified to represent scenarios of high-penetration of DERs.

A. DISSIPATIVITY

Consider the discrete time nonlinear system

$$\begin{aligned} x(k+1) &= f(x(k), u(k)) \\ y(k) &= h(x(k), u(k)), \end{aligned} \tag{15}$$

where $x(k) \in \mathbb{R}^n$ is the system state and $u(k) \in \mathbb{R}^m$ is the system input. Let f and h be real analytic about $(x = 0, u = 0)$. Without loss of generality we assume that the pair $(x = 0, u = 0)$ is an equilibrium for (15). Then, the system (15) is said to be dissipative with respective to the supply rate $w(u(k), y(k))$, if there exists a nonnegative function $S(x)$, called the storage function, satisfying $S(0) = 0$ such that

$$S(x(k+1)) - S(x(k)) \leq w(u(k), y(k)). \tag{16}$$

In particular, if (16) holds with strict inequality then (15) is *strictly dissipative*. Furthermore, (15) is called $(Q, S, R)-$dissipative if (16) holds for $w(u, y) = u^\top Ru + 2y^\top Su + y^\top Qy$, where $Q = Q^\top$, S and $R = R^\top$ are matrices with appropriate dimensions.

The following result is from [40, Corollary 1]. Consider the discrete time system (15) and its linearized model around equilibrium $(x = 0, u = 0)$. Assume that the linearized model is strictily $(Q, S, R)-$ dissipative with a storage function $S(z) = (1/2)z^\top Pz$. If

$$R + S^\top D + D^\top S + D^\top QD - B^\top PB > 0 \tag{17}$$

then system (15) is locally strictly $(Q, S, R)-$ dissipative.

B. PROOF of THEOREM 1

If the initial condition $v(0)$ satisfies $v(0) < v_l$, then the controller (4) implies that $u(0) = q_{\max}$. The state $q(1) = u(0) = q_{\max}$, which, in turn, implies from (5) that $v_l \leq v(1) \leq v_h$. Similarly, if $v(0) > v_h$, $v_l \leq v(1) \leq v_h$. Thus, for asymptotic behavior of the system, we can assume without loss of generality that the initial condition of the system satisfies $v_l \leq v(0) \leq v_h$ and the control input is given by

$$u(k) = u^\star - \overline{K}\left(v(k) - v^\star\right). \tag{18}$$

To prove part (i), we begin by simplifying (3) using the controller (18) to write

$$\begin{aligned} v(k) &= (I - X(k+1)\overline{K})\Delta v(k) \\ \omega(k) &= -(I + X(k+1)\overline{K})\Delta v(k). \end{aligned} \tag{19}$$

Further, from the definition of K in (7), we can write

$$X(k+1)\overline{K} = (I + K(k))(I - K(k))^{-1}. \tag{20}$$

We can use (20) to rewrite (19) as

$$v(k) = K(k)\omega(k). \tag{21}$$

Using Lemma 1 and (21), we have

$$S(k+1) - S(k) = v(k)^\top \omega(k) = \omega(k)^\top K(k)\omega(k). \tag{22}$$

This concludes the proof of part (i).

For part (ii), we note that since $\lim_{k\to\infty} X(k) = \overline{X}$, $K(k)$ also converges to some matrix $K < 0$ as $k \to \infty$. Then, (22) implies the following:

- If $w(\omega) = 0$, then $\omega(k) = 0$. From (21), we then obtain $v(k) = 0$. Thus, the relation (3) yields $v(k) = v^\star$ and consequently $q(k) = q^\star$.
- If $w(\omega) \neq 0$, then $S(k+1) < S(k)$. Since $X(k) > 0$, $S(k) \geq 0$, with $S(k) = 0$ if and only if $\Delta q(k) = 0$, or in other words, $q(k) = q^\star$ and $v(k) = v^\star$.

These two observations imply that the system Σ_l with (4) is asymptotically stabilized to the operating point $(q^\star, v^\star)$.

C. PROOF of THEOREM 2

Note that for the system with $J(\widehat{u_i^\star})$ as the input and $\widehat{\theta_i}$ as the output, the transfer function is given by

$$\frac{-\gamma}{z-1}[a_i\cos(w_ik)]\frac{z-1}{z+h},$$

where a transfer function in front of a bracketed time function, such as $G(z)[u(k)]$, means a time-domain signal obtained as an output of $G(z)$ driven by $u(k)$. From [41, Lemma B.5], this transfer function is exponentially stable. This implies that the state-space form of this transfer function, as given by (11)-(12), is adequate for the application of the two-time scale averaging theory [42].

Now, we write the closed loop dynamics in terms of average signals. To this end, for a signal $\kappa_i(k)$, denote the average signal of $\kappa_i(k)$, over a time-period T, by $\kappa_{i,a} := \frac{1}{T}\sum_{l=0}^{T}\kappa_i(l)$. Further, denote by $\tilde{u^\star}_i(k)$ the tracking error $\widehat{\theta}_i(k) - u_i^\star$ in $\widehat{\theta}_i(k)$ with respect to $u_i^\star$. Finally, denote

$$\phi_i(\tilde{u^\star}_i(k)) = J_i(\tilde{u^\star}_i + u_i^\star + a_i\cos(2\pi\alpha_i k)). \tag{23}$$

Note that $\phi_i(.)$ is a convex function and has a minimum at $\tilde{u^\star}_i = 0$. A Taylor series expansion thus yields

$$J(\widehat{u_i^\star}) = \phi(\tilde{u^\star}_i + a_i\cos(w_ik)) \tag{24}$$

$$= \phi(\tilde{u^\star}) + \nabla_{u^\star}\phi(\tilde{u^\star})a_i\cos(w_ik). \tag{25}$$

Using (25) and the fact that $0 < \alpha_i < 1$, we can compute

$$\frac{1}{T}\sum_{l=0}^{T} J_i(\widehat{u^\star}(l)) = \phi_{i,a}(\tilde{u^\star}_{i,a}), \tag{26}$$

$$\frac{1}{T}\sum_{l=0}^{T}\cos(2\pi\alpha_i l)J(\widehat{u^\star}(l)) = \frac{a_i}{2}\nabla_{u_i^\star}\phi_{i,a}(\tilde{u}_{i,a}^\star). \tag{27}$$

Using (26) and (27), the averaging dynamics in (10)-(12) are simplified to

$$\widehat{u_{i,a}^\star}(k+1) = \widehat{\theta_{i,a}}(k+1) \tag{28}$$

$$\widehat{\theta_{i,a}}(k+1) = \widehat{\theta_{i,a}}(k) - \frac{\gamma_i a_i^2}{2}\nabla_{u_i^\star}\phi_{i,a}(\tilde{u}_{i,a}^\star) \tag{29}$$

$$\zeta_{i,a}(k+1) = -h\zeta_{i,a}(k) + \phi_{i,a}(\tilde{u^\star}_{i,a}). \tag{30}$$

From (24) and (28), we obtain that $\nabla_{u_i^\star}\phi_{i,a}(\tilde{u}_{i,a}^\star) = \nabla_{u_i^\star}J_{i,a}(\widehat{\theta_{i,a}})$. This implies that (29) represents the gradient descent dynamics on the cost-function $J_{i,a}(\widehat{u_{i,a}^\star})$, which is convex and has a minimum at $u_{i,a}^\star$. Since $\frac{\gamma_i a_i^2}{2} < 1$, we have $\widehat{\theta_{i,a}} \to u_{i,a}^\star$, and $\phi_{i,a}(\tilde{u^\star}_{i,a}) = 0$. From (30), noting that $0 < h < 1$ we have $\zeta_{i,a}(k) \to 0$. Convergence of each component $\widehat{u_i^\star}(k)$ to a value $\overline{u}_i$ that is in an $O(a_i)$ neighbourhood of $u_i^\star$ is thus guaranteed [37], [41].

ACKNOWLEDGMENT

The authors would like to thank Dr. Imre Gyuk, the Director of the Energy Storage Program, for his continued support. This article describes objective technical results and analysis. Any subjective views or opinions that might be expressed in the article do not necessarily represent the views of U.S. Department of Energy or U.S. government. The employee owns all right, title, and interest in and to the article and is solely responsible for its contents. The U.S. government retains and the publisher, by accepting the article for publication, acknowledges that U.S. government retains a non-exclusive, paid-up, irrevocable, world-wide license to publish or reproduce the published form of this article or allow others to do so, for U.S. government purposes. The DOE will provide public access to these results of federally sponsored research in accordance with the DOE Public Access Plan (https://www.energy.gov/downloads/doe-public-access-plan).

REFERENCES

[1] F. Katiraei and J. R. Agüero, "Solar PV integration challenges," *IEEE Power Energy Mag.*, vol. 9, no. 3, pp. 62–71, May 2011.

[2] R. Seguin, J. Woyak, D. Costyk, J. Hambrick, and B. Mather, "High-penetration PV integration handbook for distribution engineers," Dept. Nat. Renew. Energy Lab. (NREL), Golden, CO, USA, Tech. Rep. NREL/TP-5D00-63114, 2016.

[3] P. N. Vovos, A. E. Kiprakis, A. R. Wallace, and G. P. Harrison, "Centralized and distributed voltage control: Impact on distributed generation penetration," *IEEE Trans. Power Syst.*, vol. 22, no. 1, pp. 476–483, Feb. 2007.

[4] G. Cavraro and R. Carli, "Local and distributed voltage control algorithms in distribution networks," *IEEE Trans. Power Syst.*, vol. 33, no. 2, pp. 1420–1430, Mar. 2018.

[5] G. Fusco and M. Russo, "A decentralized approach for voltage control by multiple distributed energy resources," *IEEE Trans. Smart Grid*, vol. 12, no. 4, pp. 3115–3127, Jul. 2021.

[6] W. Wang, N. Yu, Y. Gao, and J. Shi, "Safe off-policy deep reinforcement learning algorithm for Volt-VAR control in power distribution systems," *IEEE Trans. Smart Grid*, vol. 11, no. 4, pp. 3008–3018, Jul. 2020.

[7] A. R. D. Fazio, C. Risi, M. Russo, and M. D. Santis, "Coordinated optimization for zone-based voltage control in distribution grids," *IEEE Trans. Ind. Appl.*, vol. 58, no. 1, pp. 173–184, Jan. 2022.

[8] Z. Tang, D. J. Hill, and T. Liu, "Distributed coordinated reactive power control for voltage regulation in distribution networks," *IEEE Trans. Smart Grid*, vol. 12, no. 1, pp. 312–323, Jan. 2021.

[9] S. Bolognani and S. Zampieri, "A distributed control strategy for reactive power compensation in smart microgrids," *IEEE Trans. Autom. Control*, vol. 58, no. 11, pp. 2818–2833, Nov. 2013.

[10] S. Bolognani, R. Carli, G. Cavraro, and S. Zampieri, "On the need for communication for voltage regulation of power distribution grids," *IEEE Trans. Control Netw. Syst.*, vol. 6, no. 3, pp. 1111–1123, Sep. 2019.

[11] Y. Wang, K. T. Tan, X. Y. Peng, and P. L. So, "Coordinated control of distributed energy-storage systems for voltage regulation in distribution networks," *IEEE Trans. Power Del.*, vol. 31, no. 3, pp. 1132–1141, Jun. 2016.

[12] M. Zeraati, M. E. H. Golshan, and J. M. Guerrero, "A consensus-based cooperative control of PEV battery and PV active power curtailment for voltage regulation in distribution networks," *IEEE Trans. Smart Grid*, vol. 10, no. 1, pp. 670–680, Jan. 2019.

[13] Y. Gao, W. Wang, and N. Yu, "Consensus multi-agent reinforcement learning for Volt-VAR control in power distribution networks," *IEEE Trans. Smart Grid*, vol. 12, no. 4, pp. 3594–3604, Jul. 2021.

[14] K. E. Antoniadou-Plytaria, I. N. Kouveliotis-Lysikatos, P. S. Georgilakis, and N. D. Hatziargyriou, "Distributed and decentralized voltage control of smart distribution networks: Models, methods, and future research," *IEEE Trans. Smart Grid*, vol. 8, no. 6, pp. 2999–3008, Nov. 2017.

[15] N. Patari, A. K. Srivastava, G. Qu, and N. Li, "Distributed optimal voltage control for three phase unbalanced distribution systems with DERs," in *Proc. IEEE Ind. Appl. Soc. Annu. Meeting*, Oct. 2020, pp. 1–8.

[16] T. T. Mai, A. N. M. M. Haque, P. P. Vergara, P. H. Nguyen, and G. Pemen, "Adaptive coordination of sequential droop control for PV inverters to mitigate voltage rise in PV-rich LV distribution networks," *Electr. Power Syst. Res.*, vol. 192, Mar. 2021, Art. no. 106931.

[17] P. Jahangiri and D. C. Aliprantis, "Distributed Volt/VAr control by PV inverters," *IEEE Trans. Power Syst.*, vol. 28, no. 3, pp. 3429–3439, Aug. 2013.

[18] H. Zhu and H. J. Liu, "Fast local voltage control under limited reactive power: Optimality and stability analysis," *IEEE Trans. Power Syst.*, vol. 31, no. 5, pp. 3794–3803, Sep. 2016.

[19] F. Olivier, P. Aristidou, D. Ernst, and T. Van Cutsem, "Active management of low-voltage networks for mitigating overvoltages due to photovoltaic units," *IEEE Trans. Smart Grid*, vol. 7, no. 2, pp. 926–936, Mar. 2016.

[20] C. Lin, W. Wu, B. Zhang, B. Wang, W. Zheng, and Z. Li, "Decentralized reactive power optimization method for transmission and distribution networks accommodating large-scale DG integration," *IEEE Trans. Sustain. Energy*, vol. 8, no. 1, pp. 363–373, Jan. 2017.

[21] J. W. Simpson-Porco, F. Dörfler, and F. Bullo, "Voltage stabilization in microgrids via quadratic droop control," *IEEE Trans. Autom. Control*, vol. 62, pp. 1239–1253, Mar. 2017.

[22] J. Schiffer, R. Ortega, A. Astolfi, J. Raisch, and T. Sezi, "Conditions for stability of droop-controlled inverter-based microgrids," *Automatica*, vol. 50, no. 10, pp. 2457–2469, Oct. 2014.

[23] K. Baker, A. Bernstein, E. Dall'Anese, and C. Zhao, "Network-cognizant voltage droop control for distribution grids," *IEEE Trans. Power Syst.*, vol. 33, no. 2, pp. 2098–2108, Mar. 2018.

[24] A. Singhal, V. Ajjarapu, J. Fuller, and J. Hansen, "Real-time local Volt/VAR control under external disturbances with high PV penetration," *IEEE Trans. Smart Grid*, vol. 10, no. 4, pp. 3849–3859, Jul. 2019.

[25] K. Turitsyn, P. Sulc, S. Backhaus, and M. Chertkov, "Options for control of reactive power by distributed photovoltaic generators," *Proc. IEEE*, vol. 99, no. 6, pp. 1063–1073, Jun. 2011.

[26] F. Andrén, B. Bletterie, S. Kadam, P. Kotsampopoulos, and C. Bucher, "On the stability of local voltage control in distribution networks with a high penetration of inverter-based generation," *IEEE Trans. Ind. Electron.*, vol. 62, no. 4, pp. 2519–2529, Apr. 2015.

[27] A. Eggli, S. Karagiannopoulos, S. Bolognani, and G. Hug, "Stability analysis and design of local control schemes in active distribution grids," *IEEE Trans. Smart Grid*, vol. 36, no. 3, pp. 1900–1909, May 2021.

[28] K. De Brabandere, B. Bolsens, J. Van Den Keybus, J. Driesen, M. Prodanovic, and R. Belmans, "Small-signal stability of grids with distributed low-inertia generators taking into account line phasor dynamics," in *Proc. 18th Int. Conf. Exhib. Electr. Distrib. (CIRED)*, 2005, pp. 1–5.

[29] M. Farivar, L. Chen, and S. Low, "Equilibrium and dynamics of local voltage control in distribution systems," in *Proc. 52nd IEEE Conf. Decis. Control*, Dec. 2013, pp. 4329–4334.

[30] L. Blakely, M. J. Reno, and J. Peppanen, "Identifying common errors in distribution system models," in *Proc. IEEE 46th Photovoltaic Specialists Conf. (PVSC)*, Jun. 2019, pp. 3132–3139.

[31] K. C. Kosaraju, L. Ye, V. Gupta, R. Trevizan, B. Chalamala, and R. H. Byrne, "Dissipativity-based voltage control in distribution grids," in *Proc. IEEE Power Energy Soc. Innov. Smart Grid Technol. Conf. (ISGT)*, Apr. 2022, pp. 1–5.

[32] M. E. Baran and F. F. Wu, "Network reconfiguration in distribution systems for loss reduction and load balancing," *IEEE Power Eng. Rev.*, vol. 9, no. 4, pp. 101–102, Apr. 1989.

[33] V. Kekatos, L. Zhang, G. B. Giannakis, and R. Baldick, "Voltage regulation algorithms for multiphase power distribution grids," *IEEE Trans. Power Syst.*, vol. 31, no. 5, pp. 3913–3923, Sep. 2016.

[34] N. Li, G. Qu, and M. Dahleh, "Real-time decentralized voltage control in distribution networks," in *Proc. 52nd Annu. Allerton Conf. Commun., Control, Comput.*, Oct. 2014, pp. 582–588.

[35] H. K. Khalil, *Nonlinear Systems*, 3rd ed. New York, NY, USA: Prentice-Hall, 2002.

[36] T. Matiakis, S. Hirche, and M. Buss, "Independent-of-delay stability of nonlinear networked control systems by scattering transformation," in *Proc. Amer. Control Conf.*, Jun. 2006, pp. 1–6.

[37] J.-Y. Choi, M. Krstic, K. B. Ariyur, and J. S. Lee, "Extremum seeking control for discrete-time systems," *IEEE Trans. Autom. Control*, vol. 47, no. 2, pp. 318–323, Feb. 2002.

[38] R. C. Dugan and T. E. McDermott, "An open source platform for collaborating on smart grid research," in *Proc. IEEE Power Energy Soc. Gen. Meeting*, Jul. 2011, pp. 1–7.

[39] A. Gagné, D. Turcotte, N. Goswamy, and Y. Poissant, "High resolution characterisation of solar variability for two sites in Eastern Canada," *Sol. Energy*, vol. 137, pp. 46–54, Nov. 2016.

[40] M. Xia, P. J. Antsaklis, V. Gupta, and M. J. McCourt, "Determining passivity using linearization for systems with feedthrough terms," *IEEE Trans. Autom. Control*, vol. 60, no. 9, pp. 2536–2541, Sep. 2015.

[41] K. B. Ariyur and M. Krstic, *Real-Time Optimization By Extremum-Seeking Control*. Hoboken, NJ, USA: Wiley, 2003.

[42] E.-W. Bai, L.-C. Fu, and S. S. Sastry, "Averaging analysis for discrete time and sampled data adaptive systems," *IEEE Trans. Circuits Syst.*, vol. CS-35, no. 2, pp. 137–148, Feb. 1988.

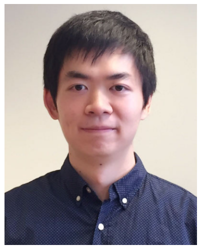

LINTAO YE received the M.S. degree in mechanical engineering and the Ph.D. degree in electrical and computer engineering from Purdue University, IN, USA, in 2017 and 2020, respectively. He is currently a Lecturer with the School of Artificial Intelligence and Automation, Huazhong University of Science and Technology, Wuhan, China. He was a Post-Doctoral Researcher with the University of Notre Dame, IN, USA. His research interests are in the areas of optimization algorithms, control theory, estimation theory, and network science.

KRISHNA CHAITANYA KOSARAJU received the master's degree in control and instrumentation and the Ph.D. degree in electrical engineering from Indian Institute of Technology Madras, in 2013 and 2018, respectively. He has been a Post-Doctoral Researcher with the University of Groningen, University of Notre Dame, and University of Clemson. His research activities are mainly in the area of nonlinear control theory, passivity based control and optimization theory with application to power networks, building systems, and reinforcement learning.

VIJAY GUPTA (Fellow, IEEE) received the B.Tech. degree in electrical engineering from Indian Institute of Technology Delhi and the M.S. and Ph.D. degrees in electrical engineering from California Institute of Technology. He is currently with the Elmore Family School of Electrical and Computer Engineering, Purdue University. His research interests are broadly at the interface of communication, control, distributed computation, and human decision making. He received the 2018 Antonio J Rubert Award from the IEEE Control Systems Society, the 2013 Donald P. Eckman Award from the American Automatic Control Council, and the 2009 National Science Foundation (NSF) CAREER Award.

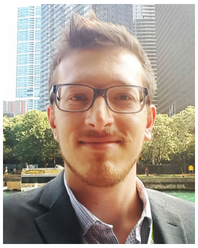

RODRIGO D. TREVIZAN (Member, IEEE) received the B.S. and M.Sc. degrees in electrical engineering from the Federal University of Rio Grande do Sul, Brazil, in 2012 and 2014, respectively, the Diplôme D'Ingénieur degree in power systems engineering from the Grenoble Institute of Technology (ENSE3) in 2011, and the Ph.D. degree in electrical and computer engineering from the University of Florida in 2018. In 2019, he joined the Energy Storage Technology and Systems Department, Sandia National Laboratories, Albuquerque, NM, USA. His research interests include cyberphysical security of energy storage systems, techno-economic analysis of energy storage, control of energy storage and demand response for power grid stabilization, and power system state estimation.

RAYMOND H. BYRNE (Fellow, IEEE) received the B.S. degree in electrical engineering from the University of Virginia, the M.S. degree in electrical engineering from the University of Colorado, the M.S. degree in financial mathematics from the University of Chicago, and the Ph.D. degree in electrical engineering from the University of New Mexico. He has been the Manager of the Power Electronics and Energy Conversion Department, Sandia National Laboratories, since 1989. Prior working as the Manager, he was a Distinguished Member of the Technical Staff. He currently serves as the Team Lead of the Equitable Regulatory Environment Thrust Area of the Sandia Energy Storage Program. Awards include Time Magazine Invention of the Year in Robotics in 2001 and the Prize Paper Award at the 2016 IEEE Power and Energy Society General Meeting. He is a member of Tau Beta Pi, Eta Kappa Nu, and Sigma Xi.

BABU R. CHALAMALA (Fellow, IEEE) received the B.Tech. degree in electronics and communications engineering from Sri Venkateswara University and the Ph.D. degree in physics from the University of North Texas. He is currently the Head of the Energy Storage Technology and Systems Department and the Program Manager of Grid Energy Storage with the Sandia National Laboratories. Prior to joining Sandia in 2015, he was a Corporate Fellow of MEMC Electronic Materials, where he led research and development and product development in grid scale energy storage for five years. He has founded two startup companies commercializing large format lithium batteries and digital X-ray sources. Earlier, he was a Research Staff Member with Motorola and Texas Instruments, where he made contributions to the development of materials and device technologies for flat panel displays and microelectronics. He has authored over 120 published articles and awarded nine U.S. patents. He is a fellow of American Association for the Advancement of Science and the National Academy of Inventors. He is also a Life Member of the Electrochemical Society and a member of the Materials Research Society. He currently serves as the Chair for Energy Storage and Stationary Battery Committee of IEEE Power and Energy Society and as a Senior Editor for IEEE ACCESS. He has served on the editorial board of the PROCEEDINGS OF THE IEEE, IEEE ACCESS, IEEE JOURNAL OF DISPLAY TECHNOLOGY AND ENERGY STORAGE JOURNAL.